

# Environmental Science Processes & Impacts

[rsc.li/espi](https://rsc.li/espi)



ISSN 2050-7887



Cite this: *Environ. Sci.: Processes Impacts*, 2024, **26**, 975

## Indoor cooking and cleaning as a source of outdoor air pollution in urban environments†

Toby J. Carter, <sup>a</sup> David R. Shaw, <sup>a</sup> David C. Carslaw<sup>b</sup> and Nicola Carslaw <sup>\*a</sup>

Indoor sources of air pollution, such as from cooking and cleaning, play a key role in indoor gas-phase chemistry. The focus of the impact of these activities on air quality tends to be indoors, with less attention given to the impact on air quality outside buildings. This study uses the INdoor CHEmical Model in Python (INCHEM-Py) and the Advanced Dispersion Modelling System (ADMS) to quantify the impact cooking and cleaning have on indoor and outdoor air quality for an idealised street of houses. INCHEM-Py has been developed to determine the concentrations of 106 indoor volatile organic compounds at the point they leave a building (defined as near-field concentrations). For a simulated 140 m long street with 10 equi-distant houses undertaking cooking and cleaning activities, the maximum downwind concentration of acetaldehyde increases from a background value of 0.1 ppb to 0.9 ppb post-cooking, whilst the maximum downwind chloroform concentrations increase from 1.2 to 6.2 ppt after cleaning. Although emissions to outdoors are higher when cooking and cleaning happen indoors, the contribution of these activities to total UK emissions of volatile organic compounds is low (less than 1%), and comprise about a quarter of those emitted from traffic across the UK. It is important to quantify these emissions, particularly as continued vehicle technology improvements lead to lower direct emissions outdoors, making indoor emissions relatively more important. Understanding how indoor pollution can affect outdoor environments, will allow better mitigation measures to be designed in the future that can take into account all sources of pollution that contribute to human exposure.

Received 14th November 2023  
Accepted 17th March 2024

DOI: 10.1039/d3em00512g  
rsc.li/espi

### Environmental significance

Household cooking and cleaning produce numerous volatile organic compounds, which can react with indoor oxidants, including OH and O<sub>3</sub> to produce harmful secondary pollutants. The resultant air pollutant formation affects indoor air quality, but less is known about its impact on the outdoor air quality around buildings. This study shows that variation in individual behaviour in identical houses can lead to significant differences in both indoor concentrations and emission rates to outdoors from individual houses. However, household cooking and cleaning activities are unlikely to be an important source of air pollution outdoors, representing only 0.85% of total UK VOC emissions.

## 1 Introduction

Air pollution exposure is classified as the fourth most important global risk factor for human health,<sup>1,2</sup> with the World Health Organisation (WHO) attributing 6.7 million deaths per year to poor outdoor and indoor air quality.<sup>3</sup> The WHO noted that household air pollution caused approximately 3.2 million of these annual deaths,<sup>3</sup> with most of these occurring in lower income countries.

The public are becoming more aware of the health effects of air pollution, especially since the COVID-19 pandemic, which has also increased media interest in the topic. Consequently,

there is heightened awareness that healthy indoor environments are important, particularly given we spend approximately 90% of our time indoors in high income countries like the UK,<sup>4</sup> where we receive most of our exposure to air pollution.<sup>5</sup>

Household activities such as cooking and cleaning contribute to indoor air pollution. Cooking can emit primary pollutants including particulate matter (ultrafine and fine), nitrogen oxides and a variety of volatile organic compounds (VOCs).<sup>6–12</sup> The inhalation of particulate matter (PM) especially, has been found to affect our cardiovascular system: the risks can be accentuated through prolonged exposure,<sup>13</sup> such as might be the case when in close proximity during the preparation of a meal, or for those working in a commercial kitchen.

Secondary pollutants can be formed indoors mainly from the gas-phase reaction of VOCs with indoor oxidants, including ozone (O<sub>3</sub>) and hydroxyl (OH) and nitrate radicals (NO<sub>3</sub>).<sup>14–20</sup> These secondary chemicals can be more harmful to human health than the primary species themselves.<sup>21,22</sup>

<sup>a</sup>Department of Environment and Geography, University of York, York, YO10 5NG, UK.  
E-mail: [nicola.carslaw@york.ac.uk](mailto:nicola.carslaw@york.ac.uk)

<sup>b</sup>Department of Chemistry, University of York, York, YO10 5DD, UK

† Electronic supplementary information (ESI) available. See DOI: <https://doi.org/10.1039/d3em00512g>



Different cooking methods including roasting, frying and grilling, all with varying chemical signatures: heating methods (*e.g.* gas *versus* electric) and food types also affect emissions.<sup>23–25</sup> Cooking oils and spices have chemical fingerprints which can often pinpoint what type of meal is being prepared.<sup>25–28</sup> For example, Davies *et al.* (2023)<sup>29</sup> attributed garlic, ginger and chilli preparation to emissions of monoterpene species, whereas increases in concentrations of eucalyptol and sesquiterpenes were observed when these spices were cooked. The same study found that alcohol mixing ratios (mostly methanol) exceeded 1500 ppb, alkane mixing ratios (mostly nonane) were approximately 170 ppb and acetaldehyde mixing ratios exceeded 70 ppb during the cooking of a chicken stir fry.<sup>29</sup> These experiments were conducted in a  $\approx 4.3 \times 2.2 \times 2.3$  m space in a shipping container, where the air change rate was  $0.77 \text{ h}^{-1}$ .

Long, straight-chain alkanes are often produced from heating oils, including octane and nonane, which are produced from rapeseed oil.<sup>29</sup> The corresponding aldehydes, octanal and nonanal, are also frequently produced from cooking fats and oils.<sup>30,31</sup> These long-chained aldehydes are currently relatively understudied in both indoor and outdoor air. Wernis *et al.* (2022)<sup>32</sup> reported that nonanal had a mean concentration (from hourly measurements taken over the course of a month) of 150 ppt in suburban Livermore (California, USA). Indoor cooking from a commercial restaurant was identified as the likely source.

Cleaning is also a major contributor to indoor air pollution. Semi-volatile organic compounds (SVOCs) and VOCs, including aromatics, alkanes and monoterpeneoids are emitted from cleaning products,<sup>33–37</sup> some of which are known to be detrimental to human health.<sup>38–40</sup> Chlorinated species are also produced from cleaning, potentially increasing the risk of an asthma attack<sup>41,42</sup> and other adverse health-effects.<sup>43,44</sup> Calderon *et al.* (2022)<sup>33</sup> discovered that gas-phase concentrations of chloroform were 1131% higher in indoor breathing zones than ambient indoor concentrations when bleach cleaning products were used. Chloroform is a suspected carcinogen and can affect the central nervous system.<sup>45</sup> During an occupational study, office workers were exposed to mixing ratios of between 14 and 400 ppm of chloroform. The health effects were reported to be jaundice, nausea, vomiting and toxic hepatitis.<sup>45–47</sup>

One of the most prominent sources of indoor pollution is from the outdoor environment.<sup>48,49</sup> Outdoor air pollution can ingress into indoor spaces including homes and offices *via* windows and doors, but also through mechanical ventilation, which is now increasingly employed in the modern construction of new buildings.<sup>50</sup> In more leaky buildings, this pollutant transport is accentuated.<sup>51</sup> However, indoor air pollutants can also move outdoors. The impact of indoor air pollutants on outdoor air quality has started to receive attention recently, with a number of studies identifying enhancements of outdoor species concentrations from emissions that had originated from indoor environments.<sup>52–54</sup> However, the details of how these indoor emissions impact the outdoor ambient atmosphere remains largely unexplored. These household emissions could have a significant impact in urban areas, particularly

those with densely packed housing and at times when many homes are emitting pollutants, for example, when cooking.

One example of indoor activities having an impact on outdoor air quality is wood stove use, particularly when numerous stoves are burning in a relatively small area, or in a valley during temperature inversions. This type of situation may lead to high local concentrations of PM<sub>2.5</sub>. For instance, PM<sub>2.5</sub> concentrations up to  $48.0 \pm 27.7 \mu\text{g m}^{-3}$  were recorded in a mountainous hollow in Slovenia,<sup>55</sup> similar to PM<sub>2.5</sub> concentrations found in more densely populated urban locations across Europe.<sup>55</sup> During wood stove use, emissions are transported to the outdoor environment through distinct plumes with high concentration gradients, compared to cooking and cleaning emissions which will diffuse through indoor-outdoor exchange at various points in a building.

McDonald *et al.* (2018)<sup>52</sup> found that volatile chemical products (VCPs) used indoors, were responsible for 39–62% of measured outdoor petrochemical VOCs, compared to only 15 to 42% from transportation. Cleaning materials are one of the six main VCP categories, however cooking pollutants could potentially have a similar effect,<sup>56–58</sup> as they are released outdoors *via* windows and cooking hoods. This paper aims to identify the VOCs that are emitted when cooking and cleaning activities occur indoors, and to evaluate the potential impact of these indicator species on outdoor air quality. In this way, we can start to understand how indoor activities may impact the ambient atmosphere.

## 2 Methods

### 2.1 The Indoor Chemical model in Python

This paper uses the indoor air chemistry model, INCHEM-Py (INdoor CHEMical model in Python).<sup>59,60</sup> This model has been recently used to provide insight into oxidant surface chemistry, VOC emissions from plastic, and domestic cooking activities indoors.<sup>29,61,62</sup> INCHEM-Py is a zero-dimensional chemical box model which provides predicted concentrations of indoor gas-phase species over time, assuming a single well-mixed spatial environment.

INCHEM-Py adopts the near-explicit Master Chemical Mechanism (MCM) v3.3.1,<sup>63</sup> which describes the tropospheric degradation of 143 VOCs, incorporating approximately 20 000 reactions and 6000 gas-phase species.<sup>64–69</sup> VOC degradation is initiated by the reaction with an oxidant<sup>70–72</sup> or (in some cases) through photolysis, forming intermediate species until carbon dioxide (CO<sub>2</sub>) and water (H<sub>2</sub>O) are formed.<sup>64</sup>

INCHEM-Py calculates indoor photolysis rates by adding the contribution from attenuated sunlight through windows, to that from indoor artificial lighting.<sup>60,73</sup> Gas-to-particle partitioning is present in INCHEM-Py,<sup>74,75</sup> but only for  $\alpha$ -pinene,  $\beta$ -pinene and limonene.

INCHEM-Py solves a system of ordinary differential equations (ODEs) to calculate the rate of change of indoor concentration over time (molecule per cm<sup>3</sup> per s) in the form:

$$\frac{dC_i}{dt} = \sum R_{ij} + (\lambda_r C_{i,\text{out}} - \lambda_r C_i) - \nu_{d_i} \left( \frac{A}{V} \right) C_i + k_t \quad (1)$$



where  $C_i$  is the indoor concentration of gas-phase species  $i$  (molecule per  $\text{cm}^3$ ).  $\Sigma R_{ij}$ , represents the sum of the reaction rates between species  $i$  and species  $j$ ,  $\lambda_r$  is the air change rate (ACR) in air changes per hour ( $\text{h}^{-1}$ ),  $C_{i,\text{out}}$  is the outdoor concentration of gas-phase species  $i$  (molecule per  $\text{cm}^3$ ).  $v_{d_i}$  is the surface deposition velocity for species  $i$  ( $\text{cm s}^{-1}$ ),  $A$  is the surface area ( $\text{cm}^2$ ), and  $V$  is the volume ( $\text{cm}^3$ ). The final term ( $k_t$ ) refers to internal emissions, where  $k_t$  denotes the emission rate of species  $i$  at time  $t$  (molecule per  $\text{cm}^3$  per s). The model is described in detail in Shaw *et al.* (2023).<sup>60</sup>

A new development to INCHEM-Py (v1.2 (ref. 60)) is the addition of primary emissions from common indoor materials. Wood and paint are commonly found in homes, and are known to emit indoor air pollutants, primarily short and long-chained aldehydes.<sup>76–86</sup> New furniture often produces higher emissions of these species, which tend to decrease as it ages.<sup>76,79</sup> Published emission rates from wood and paint for formaldehyde, acetaldehyde, propanal, butanal, pentanal, hexanal, heptanal, octanal, nonanal and decanal<sup>76,79,81</sup> have been averaged and added into the model informed by the surface-area to volume ratio of wooden and painted materials in a typical kitchen,<sup>29,61,87</sup> and are provided in Table S1.† These aldehyde emission rates are assumed to remain constant throughout the simulation. Surface-specific oxidant deposition initiated emissions are also present in the model for ozone and hydrogen peroxide, as outlined in Carter *et al.* (2023)<sup>61</sup> and Shaw *et al.* (2023).<sup>60</sup> The model does not consider resuspension from surfaces.

## 2.2 Near-field concentration development

For this work, we have added a near-field gas-phase concentration, ( $C_{i,\text{nf}}$ ) (molecule per  $\text{cm}^3$ ), for 106 VOCs and methane (Table S2†) to INCHEM-Py, which represents the concentration of a species,  $i$ , as it moves from indoors to outdoors. This enables the concentration of an indoor air pollutant to be tracked as it leaves a building.  $C_{i,\text{nf}}$  is determined by the balance between formation and loss mechanisms, as shown in eqn (2). The formation of the near-field species is effectively determined by the exit rate of a species from indoors, the product of its indoor concentration ( $C_i$ ), and the air change rate ( $\lambda_r$ ). The loss rate is dependent on both chemical and physical losses. Chemical losses happen *via* photolysis and also by reactions with the hydroxyl radical ( $\text{OH}$ ) and ozone ( $\text{O}_3$ ), whilst we assume physical loss is driven by the rates of dispersion ( $k_{\text{disp}}$ ) and outdoor deposition ( $d_{i,\text{out}}$ ).

$$\frac{dC_{i,\text{nf}}}{dt} = \lambda_r C_i - k_{\text{chem}} C_{i,\text{nf}} - k_{\text{disp}} C_{i,\text{nf}} - d_{i,\text{out}} \quad (2)$$

The chemical loss rate for the near-field species as they move outdoors is calculated off-line, based on the rate coefficients in the MCM<sup>64</sup> and assuming realistic outdoor concentrations of the oxidants.<sup>60</sup> For loss *via* photolysis once the species pass outdoors, the outdoor photolysis rates are calculated in INCHEM-Py, but without applying an attenuation factor as we would to calculate indoor photolysis rates. Note that we are only interested in the near-field concentration changes, not the impact on outdoor air pollutant concentrations.

The dilution rate due to dispersion was calculated using the Advanced Dispersion Modelling System (ADMS).<sup>88</sup> ADMS is used to simulate the dispersion of air pollutant emissions from sources such as roads, chimney stacks and buildings.<sup>89</sup> The ADMS simulation assumed a typical house-sized building (10 m  $\times$  10 m  $\times$  5 m, represented as a volume source) and used meteorological conditions based on hourly data from London Heathrow in 2019. ADMS predicts the concentration of an air pollutant as a function of distance from the building, hence providing a rate of dispersion.<sup>88</sup> In this case, the unit emission of a non-reactive tracer was used, which provides the basis of dispersion for the other VOCs in the model. The fall-off in concentration was calculated from the eastern edge of the building extending in a west-east direction out to 200 m from the building facade *i.e.* approximately downwind of the prevailing wind direction (see Table S3 and eqn (S1) in the ESI†).

Physical loss owing to irreversible deposition is driven by the outdoor surface deposition velocities calculated for an average urban surface as described in Carslaw *et al.* (2007)<sup>90</sup> and assuming a constant boundary layer height (BLH) of 1000 m. The outdoor surface deposition velocities vary by species and the non-oxygenated VOCs are assumed not to undergo deposition.<sup>60</sup> The boundary layer height is assumed to be constant in our simulations and used only for the calculation of outdoor deposition rates. Emission from the houses is the major controlling factor for the near-field concentrations under our simulated conditions.

## 2.3 Cooking & cleaning emission rates

For typical cooking and cleaning emissions, the model has been informed by the HOMEChem (The House Observations of Microbial and Environmental Chemistry) experimental field campaign performed in the University of Texas at Austin test-house facility in June 2018.<sup>91</sup> The campaign focused on the impacts that human activities had on chemical transformations in the indoor environment, including the quantification of indoor air pollutant concentrations following various cooking,<sup>92,93</sup> cleaning,<sup>73,94,95</sup> ventilation and human occupancy experiments.<sup>23,96,97</sup>

For this work, we focused on the 25th June, which was considered a 'layered day'. A layered day attempts to replicate a standard day in the home, with three cooked meals and a solitary cleaning experiment.<sup>91</sup> During these experiments, the VOCs were measured using PTR-TOF-MS<sup>98,99</sup> and Iodide-CIMS<sup>100</sup> instruments. The emission rates for the detected VOCs emitted from the separate cooking and cleaning events were implemented into INCHEM-Py as timed emissions (eqn (1)) as provided in Table S4.† These emission rates were back-calculated from concentration measurements.

## 2.4 Model simulations and assumptions

**2.4.1 Layered day analysis simulation.** The model was parameterised to replicate a house situated in suburban London (latitude of 51.45 °N) in the United Kingdom. The temperature, relative humidity and air change rate of the property was assumed to be 19.9 °C, 53.8% (ref. 101) and 0.5  $\text{h}^{-1}$ ,<sup>102</sup> as outlined in Carter *et al.* (2023).<sup>61</sup> The date of the



simulation was the 21st June 2023, a photochemically active day. The date and latitude used in the model determine the solar zenith angle used to calculate outdoor photolysis rates, which are then attenuated depending on glass type to calculate indoor photolysis rates.<sup>60,73</sup>

The window panel was assumed to consist of glass with a transmission range of between 315 to 800 nm (Glass C in Blocquet *et al.* (2018)<sup>103</sup>). The outdoor concentrations for O<sub>3</sub>, nitric oxide (NO) and nitrogen dioxide (NO<sub>2</sub>) are based on measurements made at a monitoring station ('GB0586A, suburban London, 0.070766 51.45258') in suburban London,<sup>104</sup> and follow a diurnal profile in the model. The OH outdoor mixing ratios are also diurnal and have an average concentration of  $1.5 \times 10^6$  molecules per cm<sup>3</sup> over a 24 hour period. Outdoor OH has negligible impact on indoor concentrations due to the short lifetime of the OH radical. Full diurnal profiles of these species are described in Shaw *et al.* (2023).<sup>60</sup> Diurnal profiles for outdoor O<sub>3</sub>, NO and NO<sub>2</sub> are also given in Fig. 2. The outdoor VOC concentrations are set as described in Shaw *et al.* (2023)<sup>60</sup> and the outdoor concentration of carbon monoxide is assumed to be 195 ppb.<sup>104</sup> The outdoor VOC concentrations are averages based on available literature and are given in Table S5.†

Based on the HOMEChem emission rates (Table S4†), we have simulated a standard day spent in the home. A full-English breakfast (fried sausages, eggs and tomatoes) is cooked at 7:30am (till 7:46am), a vegetable stir-fry lunch at 12 noon (till 12:29pm) and a chili con carne dinner at 6pm (till 7:02pm). A chlorine-based cleaning activity occurred after lunch at 2:00pm

(till 2:13pm). It should be noted that a pilot light on the stove emitted high levels of propane during the cooking periods in the HOMEChem study,<sup>91</sup> from a possible fuel leak. Table S6† details the average percentage change of key indoor species during a day if propane emissions were omitted from the study. We found that OH and HO<sub>2</sub> radical concentrations decrease (−5 and −21% respectively), whereas RO<sub>2</sub> concentrations increase (52%) if propane is omitted.

The simulations take place in a kitchen, with a total surface area of 63.3 m<sup>2</sup> and an internal volume of 25.0 m<sup>3</sup>. The overall surface area to volume ratio (SA/V) in the kitchen is 2.53 m<sup>−1</sup> based on the measurements from Manuja *et al.* (2019)<sup>87</sup> and calculations from Carter *et al.* (2023).<sup>61</sup> The surface area to volume ratios for soft fabric, paint, skin, wood, metal, concrete, paper, plastic and glass are defined in Carter *et al.* (2023)<sup>61</sup> for the simulated kitchen. It is assumed that one adult (2 m<sup>2</sup> of skin) is present in the kitchen. We have included emission rates from breath according to Kruza *et al.* (2019)<sup>105</sup> and Weschler *et al.* (2007).<sup>106</sup>

**2.4.2 Ten-house analysis simulations.** The ten-house houses analysis assumes ten houses, 5 m apart, to replicate a typical detached row of houses. These ten houses were randomly assigned different air change rates, inhabitants and cooking and cleaning times. The street length was 140 m and each house was assumed to be 10 m × 10 m × 5 m. A ten-house ensemble provides a reasonable representation of the variation in day-to-day lifestyles and routines, providing an opportunity to vary air exchange rates, surfaces, meal times and occupancy

Table 1 The simulation conditions for the ten-house analysis

Parameter	House 1	House 2	House 3	House 4	House 5
ACR (h <sup>−1</sup> )	0.5	0.2	2.0	1.5	0.2
Lights on	7am	7am	7am	7am	No lights
Lights off	7pm	7pm	7pm	7pm	No lights
AV (cm <sup>−1</sup> )	0.0269	0.0253	0.0253	0.0253	0.0245
Human AV (cm <sup>−1</sup> )	0.0024	0.0008	0.0008	0.0008	0
Adults	2	1	1	1	0
Children	2	0	0	0	0
Breakfast (time of day)	7:30–7:46	No	7:30–7:46	7:30–7:46	No
Lunch (time of day)	12:00–12:29	12:00–12:29	No	12:00–12:29	No
Dinner (time of day)	18:00–19:02	18:00–19:02	18:00–19:02	No	No
Cleaning (time of day)	14:00–14:13	14:00–14:13	14:00–14:13	14:00–14:13	No
Parameter	House 6	House 7	House 8	House 9	House 10
ACR (h <sup>−1</sup> )	0.5	1.2	0.7	0.5	1.0
Lights on	7am	7am	7am	7am	7am
Lights off	7pm	7pm	7pm	7pm	7pm
AV (cm <sup>−1</sup> )	0.0253	0.0253	0.0269	0.0257	0.0245
Human AV (cm <sup>−1</sup> )	0.0008	0.0008	0.0024	0.0012	0.0008
Adults	1	1	2	1	1
Children	0	0	2	1	0
Breakfast (time of day)	7:30–7:46	9:30–9:46	7:30–7:46	7:30–7:46	7:30–7:46
Lunch (time of day)	12:00–12:29	14:00–14:29	12:00–12:29	12:00–12:29	12:00–12:29
Dinner (time of day)	18:00–19:02	18:00–19:02	20:00–21:02	18:00–19:02	18:00–19:02
Cleaning 1 (time of day)	8:00–8:13	15:00–15:13	14:00–14:13	14:00–14:13	No
Cleaning 2 (time of day)	14:00–14:13	—	—	—	—
Cleaning 3 (time of day)	20:00–20:13	—	—	—	—





Fig. 1 A schematic of the ten-house analysis replicating a typical row of detached houses in the UK. The airflow is assumed to be along the length of the street.

to cover a range of scenarios balanced against model complexity and runtime. The conditions and input parameters for each house are described in Table 1. The temperature, relative humidity, latitude, date, surface-specific surface area-to-volume ratios (except for human surfaces)<sup>87</sup> and glass type are the same as for the layered day simulation (described in Section 2.4.1). The air change rate distributions are based on Nazaroff (2021).<sup>102</sup> Where indoor artificial lighting is present (lights on), LED lighting was used.<sup>73</sup> A wind speed of  $2\text{ ms}^{-1}$  along the street is assumed, with the pollution emitted from the centre of each house. The wind is assumed to blow along the length of the row of houses, as demonstrated by the schematic in Fig. 1.

### 3 Results & discussion

#### 3.1 Simulated indoor air pollutant concentrations following cooking & cleaning

The diurnal profiles of key indoor species ( $\text{OH}$ ,  $\text{O}_3$ ,  $\text{NO}$ ,  $\text{NO}_2$ ,  $\text{HO}_2$ ,  $\text{RO}_2$  and  $\text{CH}_3\text{CHO}$ ) following cooking and cleaning are shown in Fig. 2. Cooking had a minimal effect on the  $\text{OH}$  concentration. The indoor  $\text{OH}$  concentration an hour before cleaning (1:00pm) was  $2.8 \times 10^5$  molecule per  $\text{cm}^3$ . During the cleaning event however,  $\text{OH}$  reached a maximum concentration of  $3.4 \times 10^6$  molecule per  $\text{cm}^3$  at 2:01pm, caused by photolytic degradation of hypochlorous acid ( $\text{HOCl}$ ), producing both  $\text{OH}$  and chlorine radicals *via* homolytic cleavage, shown in (3).<sup>107</sup> One minute after cleaning had ended (2:14pm), the indoor concentration of the  $\text{OH}$  radical was  $6.8 \times 10^5$  molecule per  $\text{cm}^3$ .



Fig. S1† gives an expanded view of the concentrations during the cleaning event. Cleaning caused a  $\approx 1200\%$  increase in  $\text{OH}$  radical concentrations.  $\text{OH}$  then quickly returns to a background level, through consumption by indoor VOCs.

Acetaldehyde concentrations were enhanced by approximately 1.02, 1.1 and 1.3 times during breakfast, lunch and dinner respectively, where the maximum acetaldehyde mixing ratios during these periods were 9.5, 10.4 and 12.1 ppb respectively, driven primarily by emissions from hot cooking oils. The background value was 9.3 ppb. Our cooking simulations didn't reach the acetaldehyde levels of 70 ppb witnessed by Davies *et al.* (2023)<sup>29</sup> during a chicken stir-fry, indicating possible emission of acetaldehyde from the cooking of chicken. Acetaldehyde reaches a maximum mixing ratio of 13.9 ppb

during the cleaning event, which is an enhancement of 1.5 times from the background value.

$\text{O}_3$  acts as a strong oxidant in the indoor environment, reacting with unsaturated VOCs produced by cooking and cleaning *via* ozonolysis reactions. The indoor diurnal profile of  $\text{O}_3$  is also dictated by ingress from outdoors. During cleaning, the ozone mixing ratio increased by 45% and reached a maximum mixing ratio of 4.9 ppb at 2:30pm.

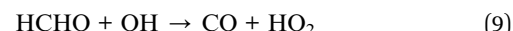
At 9:10am,  $\text{NO}$  and  $\text{NO}_2$  increase to 4.4 ppb and 1.1 ppb respectively (from 1.2 ppb and 0.7 ppb at 6am). These early morning peaks are caused by cooking but also from increased  $\text{NO}_x$  concentrations outdoors during rush-hour, creating an accumulation of  $\text{NO}_x$  indoors. Cleaning causes a change in the form of  $\text{NO}_x$ , where during the first two minutes,  $\text{NO}$  decreases (by 94%), as  $\text{NO}_2$  concentration increases (by 120%). This change is partially caused by enhanced concentrations of  $\text{HO}_2$  available to react with  $\text{NO}$ , to form  $\text{OH}$  and  $\text{NO}_2$  (4). Peroxy radical ( $\text{RO}_2$ ) concentrations are also enhanced, reacting with  $\text{NO}$  to form alkoxy radicals ( $\text{RO}$ ) and  $\text{NO}_2$  (5), the latter of which is then photolysed to make  $\text{O}_3$  (6) and (7). Since  $\text{NO}$  readily depletes  $\text{O}_3$ , the reduced levels of  $\text{NO}$  allows  $\text{O}_3$  to accumulate.



$\text{HO}_2$  and  $\text{RO}_2$  significantly increase with chlorine-based cleaning;  $\text{HO}_2$  increased from a background mixing ratio of 2.3 ppt to 61.4 ppt over one minute, with  $\text{RO}_2$  increasing from a background mixing ratio of 3.2 ppt to 2548 ppt over 12 minutes. The sudden rise in  $\text{HO}_2$  stems from the alkoxy radicals ( $\text{RO}$ ) reacting with oxygen ( $\text{O}_2$ ), through a hydrogen-migration reaction to form a carbonyl ( $\text{RCHO}$ ) and  $\text{HO}_2$  (8).<sup>108,109</sup>



$\text{HO}_2$  is also produced from the reaction of  $\text{OH}$  with formaldehyde (9). The increase in  $\text{RO}_2$  is due to the reaction of VOCs with  $\text{OH}$  (10).



The chlorine-based cleaning has a much greater effect on the indoor species in Fig. 2 compared to cooking under our simulated conditions, owing to the high concentrations of  $\text{OH}$ ,  $\text{HO}_2$  and  $\text{RO}_2$  produced from the resultant chlorine chemistry, which continued to drive indoor gas-phase reactions post-cleaning. The high  $\text{OH}$  concentrations resulted in further reactions with VOCs to form  $\text{HO}_2$  and  $\text{RO}_2$  for some time after cleaning had ceased.  $\text{HO}_2$  and  $\text{RO}_2$  did not return to baseline levels until approximately 3.5 and 5 hours respectively after the cleaning had finished.

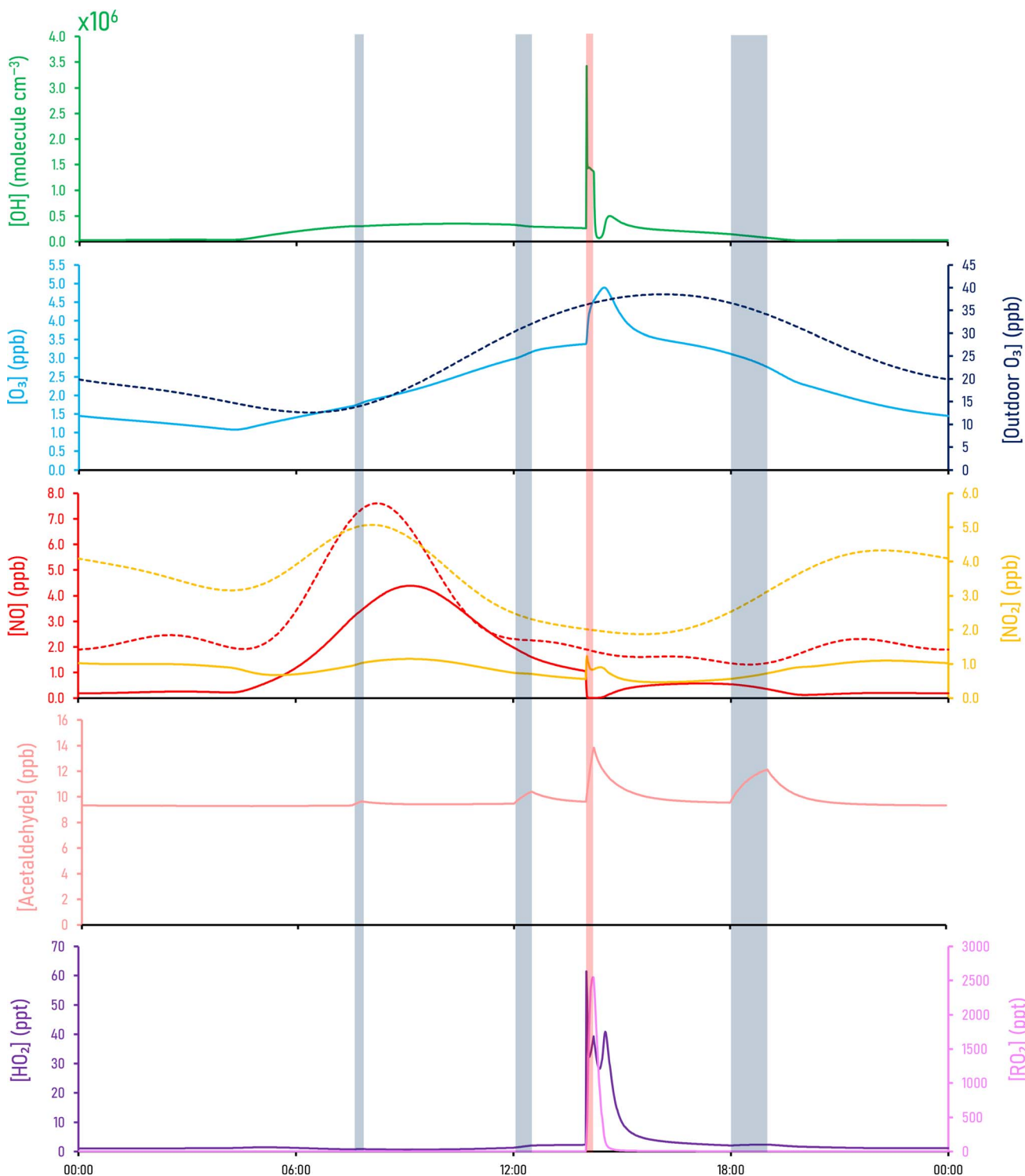


**Fig. 2** The concentrations of key indoor species in the kitchen over the duration of a typical day spent in the home. The grey shaded areas indicate periods of cooking, and the red shaded area indicates a chlorine cleaning period. The outdoor concentrations of NO (red), NO<sub>2</sub> (orange) and O<sub>3</sub> (dark blue) are shown as dashed lines on the graph.

### 3.2 Temporal variability of indoor concentrations

Indoor air pollutant concentrations vary depending on a range of factors, such as time of day, location, and indoor activities. This section considers ten different houses with varying lifestyle

routines (as described in Section 2.4.2). The range of concentrations from these ten houses at different points during the day are shown in Fig. 3, to better understand how concentrations might vary indoors according to different routines and conditions.

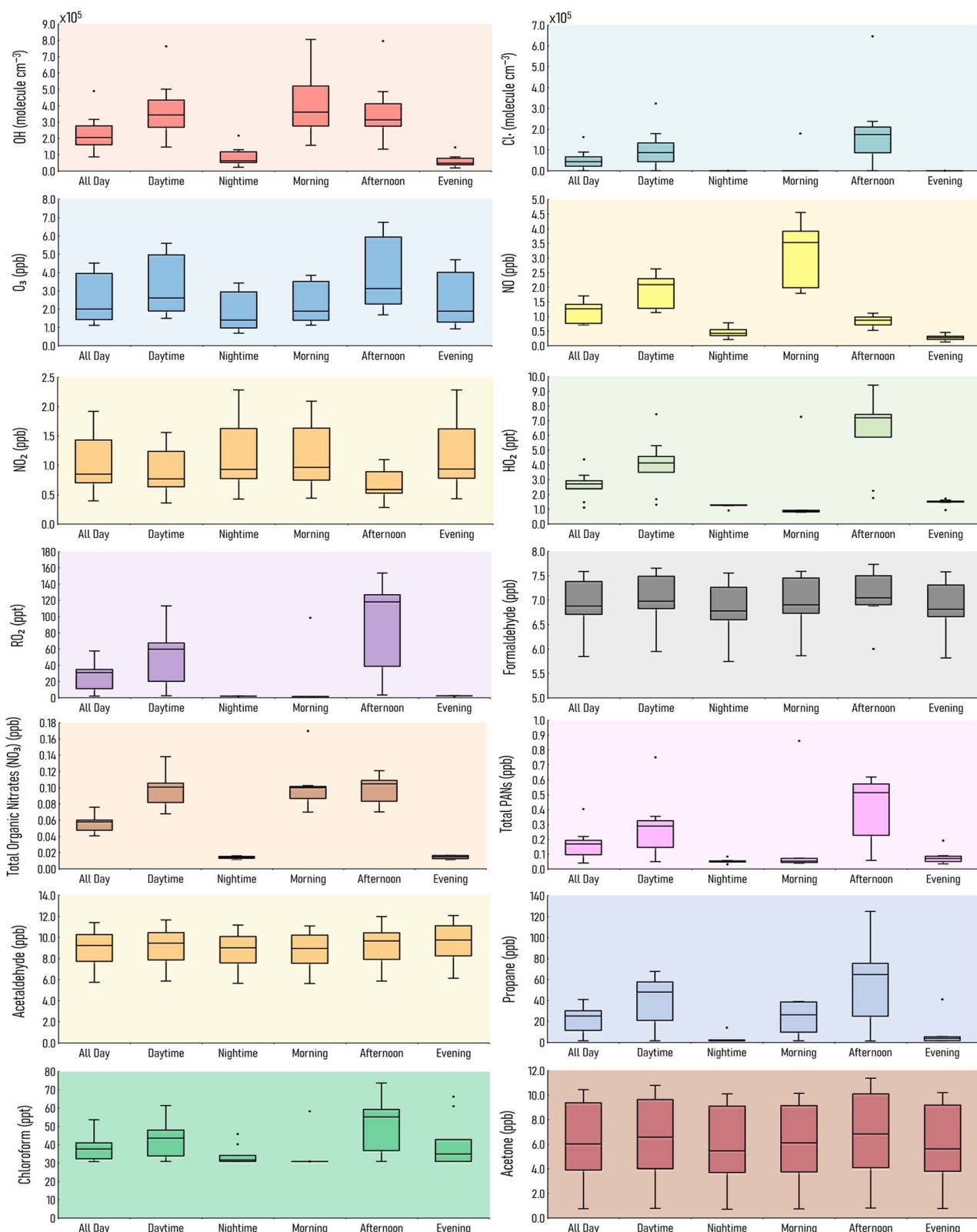
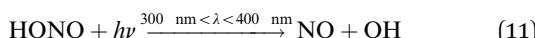


**Fig. 3** Concentrations of key indoor species from ten different houses, showing the median, the upper (75%) and lower (25%) percentiles and the upper ( $Q3 + 1.5 \times IQR$ ) and lower whiskers ( $Q1 - 1.5 \times IQR$ ). The small circles represent values which lie outside of the upper and lower whisker range. The denoted time periods are: all day (12am to 12am), daytime (7am to 7pm), nighttime (7pm to 7am), morning (6am to 12pm), afternoon (12pm to 6pm) and evening (6pm to 10pm).



The OH concentrations are lowest during nighttime and the evening. OH and NO are highest during daytime, indicating a role for photochemistry. For instance, NO and OH can be formed *via* the photolysis of HONO (11).



The median OH concentration for the full day (24 hour average) is  $2.0 \times 10^5$  molecule per  $\text{cm}^3$ . However, House 3 is an outlier, with an all day concentration of more than double at  $4.9 \times 10^5$  molecule per  $\text{cm}^3$ . It is assumed that the House 3 occupants do not cook lunch, and there is a relatively high air change rate ( $2 \text{ h}^{-1}$ ).

$\text{RO}_2$  and chlorine radical concentrations are highest in the afternoon, since this is when cleaning occurs in our simulations. Average afternoon chlorine radical concentration in House 3 reaches  $6.5 \times 10^5$  molecule per  $\text{cm}^3$ , which is higher than House 6 who clean three times a day, indicating that the high air change rate from House 3 plays an important factor in the high Cl and OH concentrations.

Formaldehyde shows little diurnal variation. House 5 has the highest average formaldehyde mixing ratio over the course of a day (7.6 ppb), but in the absence of cooking or cleaning since this house is presumed empty. However, it is also assumed to have a low air change rate ( $0.2 \text{ h}^{-1}$ ), allowing emissions from building materials to accumulate. House 3 has the lowest average formaldehyde mixing ratio over the course of a day (5.9 ppb), as it is lost outdoors owing to a relatively high air change rate.

$\text{HO}_2$  mixing ratios are highest during the day, with a median value of 2.7 ppt. Outliers which are lower than the median result are for House 10 (1.5 ppt) and House 5 (1.1 ppt). There is no cleaning in House 5 as it is empty. There is no cleaning in House 10, but the occupants still cook breakfast, lunch and dinnertime meals. House 6 has the highest all day concentration of 4.4 ppt, due to three cleaning sessions post cooking.

The main precursor for organic nitrate ( $\text{RNO}_3$ ) formation is primarily from reaction of OH with VOCs to form  $\text{RO}_2$  radicals, which then react with NO to form organic nitrates ( $\text{RNO}_3$ ) (12b). This route however, is the minor pathway ( $\leq 20\%$ ), with formation of an alkoxy radical ( $\text{RO}$ ) more likely ( $\geq 80\%$ ) (12a).

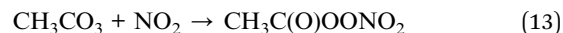


Organic nitrates can also form from the reaction of chlorine radicals with alkanes and the subsequent reaction of  $\text{RO}_2$  with NO, following the same reaction scheme as outlined above in (12a) and (12b).

Total organic nitrate ( $\text{NO}_3$ ) levels are highest during the day, as they are primarily formed by the chlorine cleaning. House 6 has a higher mixing ratio compared to the other houses (0.2 ppb), where cleaning happens after every meal, resulting in elevated total organic nitrate levels during and shortly after these cleaning periods. Since cleaning generally occurs during

daylight hours, total organic nitrate mixing ratios are higher during the day (0.1 ppb) than they are at nighttime (0.01 ppb).

Peroxyacetyl nitrate (PAN) is formed by the reaction of the acetylperoxy radical ( $\text{CH}_3\text{CO}_3$ ) with  $\text{NO}_2$  (13). Acetyl peroxy radicals are formed *via* photochemical degradation of aldehyde species, with each acetyl peroxy radical forming a distinct PAN species, which we then sum to find the total PAN concentration.



Total PANs follow a similar trend to total organic nitrate concentrations, where the median mixing ratio during the day is 0.3 ppb compared to 0.1 ppb at night. House 6 has the highest total PANs mixing ratio during the daytime (0.8 ppb) due to the extra cleaning that takes place in this house. Davies *et al.* (2023)<sup>29</sup> reported total PANs and total organic nitrate mixing ratios of approximately 50 and 60 ppt respectively during a simulated stir fry activity. Harding-Smith *et al.* (2024),<sup>37</sup> reported the total PANs mixing ratio from a scented surface cleaning product was, on average, 25 ppt over 3 hours. Total PAN concentrations increased as a result of any cleaning activity, whilst, total organic nitrate concentrations varied depending on which cleaning product was used.

Acetaldehyde mixing ratios stay fairly constant throughout the day, and show little fluctuation. There are no outliers for acetaldehyde, indicating this VOC does not reach unusually high mixing ratios. Average acetaldehyde levels in the evening reach 12.1 ppb in House 2, which is the highest of the chosen time periods. Acetone follows a similar trend to acetaldehyde, where there is little diurnal variation. However, the range of acetone mixing ratios is higher than for acetaldehyde. For example, acetone levels in the afternoon in House 4 reach 11.4 ppb, but are only 0.8 ppb in House 5. Propane levels are highest in the afternoon, predominantly from lunchtime cooking, where the mixing ratio in House 2 reaches a maximum of 125 ppb in the afternoon. Chloroform mixing ratios are dictated by cleaning activities. House 5 has the lowest average all-day chloroform mixing ratio (due to the lack of cleaning in this house) at 30.7 ppt. This increases to 53.5 ppt in House 6, which has three cleaning events over the course of that day.

### 3.3 How indoor sources contribute to outdoor air pollution

Fig. 4 shows the enhancement of emission rates from indoors to outdoors of a selection of VOCs during cooking (the three meals are averaged to one emission rate) and cleaning, over background conditions (with no cooking and cleaning activities). These emission rates are taken from the one house layered day simulation (Section 2.4.1), with the cooking and cleaning considered in separate model runs. This separation was enforced to identify which VOCs were associated with the different activities. When cooking and cleaning activities are simulated in the same model day, there is some crossover between the two activities.

The increase in emission rate of propane is the highest relative to the other VOCs, and it was highest during the cooking (approximately  $56.3 \text{ mg h}^{-1}$ ). Isobutane showed a similar pattern and is another good indicator for cooking with gas.



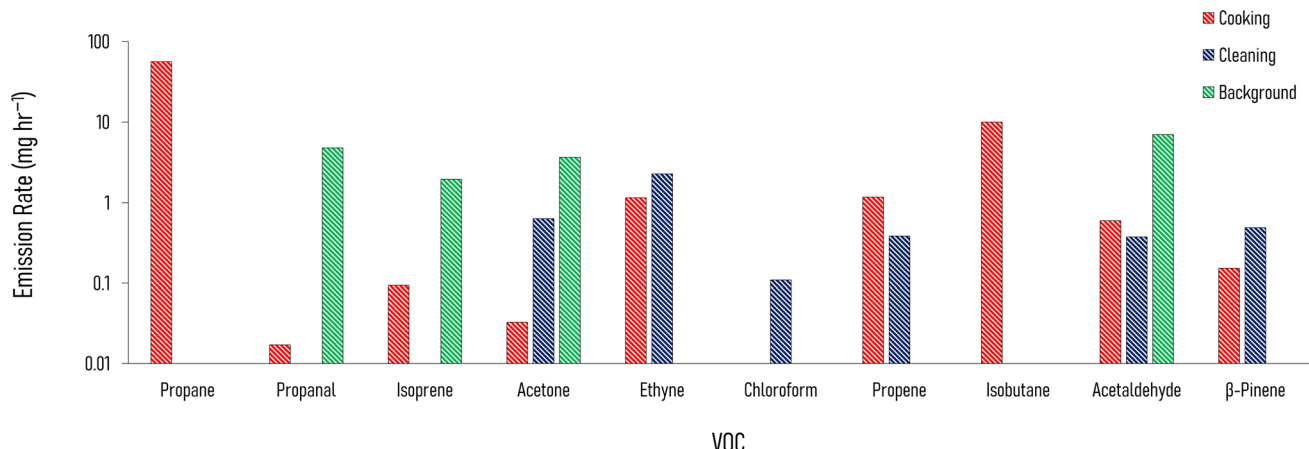


Fig. 4 The enhancement in emission rates from indoors to outdoors over background values for a variety of VOCs ( $\text{mg h}^{-1}$ ) during cooking and cleaning, from the house described in Section 2.4.1. The background emission rates are shown for comparison, and comprise of emissions from building and furnishing materials and from people.

Relatively high increases in emission rates follow cleaning for acetone ( $0.6 \text{ mg h}^{-1}$ ), ethyne ( $2.3 \text{ mg h}^{-1}$ ), and chloroform ( $0.1 \text{ mg h}^{-1}$ ). The emission rate of propene is also enhanced following cleaning ( $0.4 \text{ mg h}^{-1}$ ), but there is a larger enhancement following cooking ( $1.2 \text{ mg h}^{-1}$ ). Some of the VOCs, such as acetone and acetaldehyde are emitted outdoors from cooking, cleaning and background activities. Therefore, emission rates from the different species, or the ratio of these, can be used to understand indoor activities.

In an urban environment, there are often densely-packed houses. These houses all have the potential to emit

pollutants, primarily from cooking and cleaning activities, which can potentially affect other homes in the nearby vicinity depending on conditions. Fig. 5 shows the simulated maximum downwind concentrations of 4 VOCs (acetaldehyde, propane, chloroform and acetone), at different times of the day along the idealised ten house street (as described in Section 2.4.2). Average near-field background mixing ratios without cooking or cleaning for acetaldehyde, propane, chloroform and acetone were 0.1 ppb, 0.02 ppb, 0.4 ppt and 0.4 ppb respectively.

Acetaldehyde has the highest maximum downwind concentration at 7pm, from the chilli con carne cooking, whereas

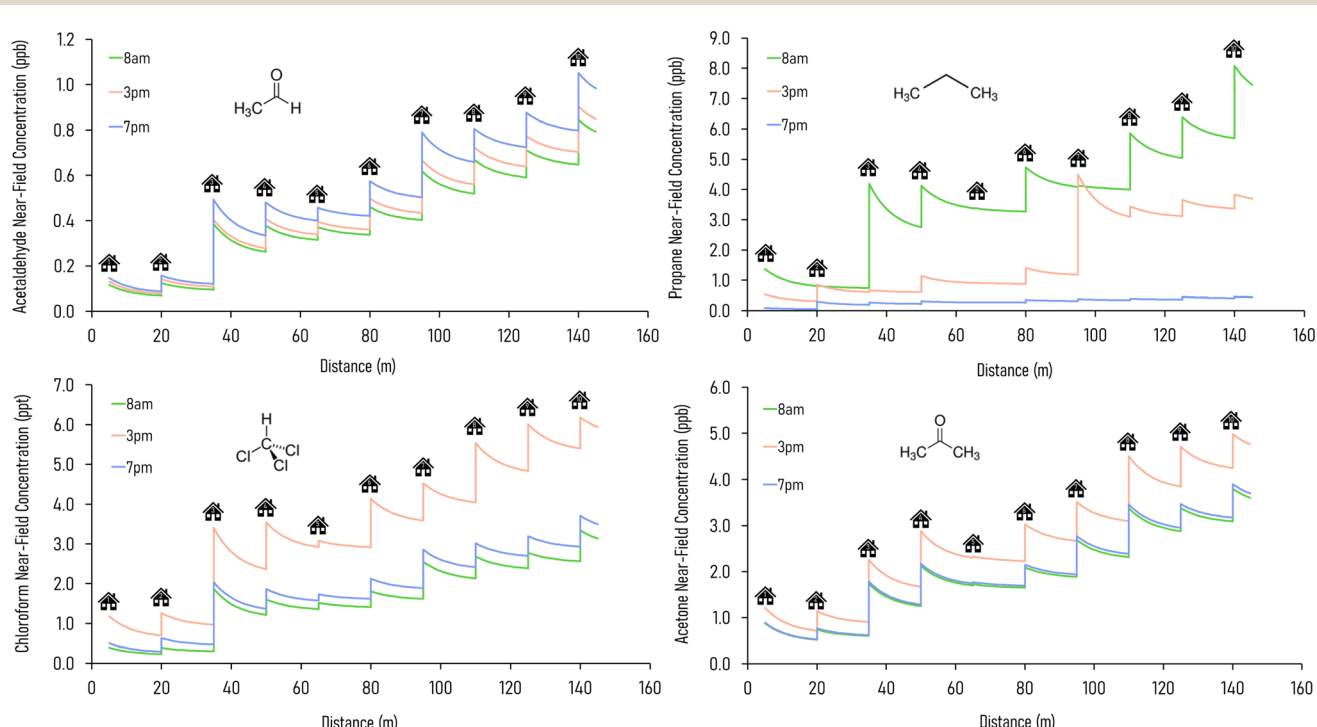


Fig. 5 The cumulative near-field concentrations of acetaldehyde (ppb), propane (ppb), chloroform (ppt) and acetone (ppb) along a street of ten houses at 8am, 3pm and 7pm. The concentration at the 10th house is the maximum downwind concentration.



propane is highest at 8am due to stove use for the full-English breakfast cooking. Chloroform and acetone are highest at 3pm, as a result of cleaning. Along the 140 m street, the maximum downwind acetaldehyde concentration increases by 629, 592 and 618% at 8am, 3pm and 7pm respectively between the first and last houses. The highest increase in near-field acetaldehyde concentration occurs at 7pm from House 3 (increase of 0.4 ppb), which is assumed to have a higher air change rate in the simulations. House 10 also has a notable increase in near-field concentration (0.3 ppb) at 7pm: the occupants of this house cook all three meals but do not clean, therefore cooking without cleaning leads to higher acetaldehyde concentrations.

The maximum downwind propane concentration increases by 488, 619 and 417% at 8am, 3pm and 7pm respectively between the first and last houses in the street. The highest increase (3.4 ppb) in near-field propane concentration occurs at 8am from House 3, again due to the higher air change rate. House 7 also provides a notable increase in near-field propane concentration (3.3 ppb) at 3pm, owing to a later lunch (at 2pm).

The maximum downwind chloroform concentration increases by 754, 422, 644% at 8am, 3pm and 7pm respectively, primarily from the chlorine cleaning. The highest increase in near-field chloroform concentration occurs at 3pm from House 3 (increase of 2.4 ppt). There are smaller increases in near-field chloroform at 8am and 7pm as cleaning occurs mostly in the afternoon in the ten-house analysis. House 8 also has a notable increase in near-field chloroform (1.5 ppt) at 3pm. House 8 is cleaned at the same time as most other houses (2pm), but dinner is not prepared until 8pm. This indicates that there is a smaller increase in near-field chloroform when food, in this case a chilli con carne, is being cooked and prepared.

Finally, the maximum downwind acetone concentration increases by 334, 311, 338% at 8am, 3pm and 7pm respectively, with a smaller variation over time than for the other species. The lower variation is due to a constant source of indoor acetone from the occupants (skin and breath). The highest increase in near-field acetone concentration occurs at 3pm from House 3 (increase of 1.4 ppb), owing to a higher air change rate. House 5 shows little increase in near-field acetone concentration during the day (0.02–0.03 ppb) as it is empty.

A comparative analysis simulated a more densely-packed street, where houses are terraced with no gap between them. This analysis uses the same ten-house conditions as described in Section 2.4.2, but the length of the street was assumed to be 100 m. The increase in maximum downwind acetaldehyde concentration from House 1 to House 10 at 8am was 648% which is slightly higher than the 629% increase in the detached house street. The percentage increase in maximum downwind concentration of acetone at 7pm on the terraced street was 351%. The percentage increase of maximum downwind propane and chloroform across the terraced street was highest at 3pm and 8am (639 and 776% respectively). The overall increase over the ten houses for the detached and the terraced streets at 8am, 3pm and 7pm for maximum downwind acetaldehyde, propane, chloroform and acetone are given in Table 2.

**Table 2** The maximum downwind concentration increases of acetaldehyde (ppb), propane (ppb), chloroform (ppt) and acetone (ppb) on a detached (D) (140 m) and terraced (T) street (100 m) from the ten-house analysis

Time of day	Acetaldehyde	Propane	Chloroform	Acetone
8am (D)	0.7	6.7	3.0	2.9
3pm (D)	0.8	3.3	5.0	3.8
7pm (D)	0.9	0.4	3.2	3.0
8am (T)	0.8	6.9	3.0	3.0
3pm (T)	0.8	3.4	5.2	3.9
7pm (T)	0.9	0.4	3.3	3.1

This indicates that due to the closer proximity of the houses, there is a higher maximum downwind concentration of the emitted VOCs for terraced housing than detached housing, however this increase is minimal. House 3 was the biggest emitter of VOCs due to its higher ventilation rate, whereas House 5 was the lowest emitter both due to its lower ventilation rate but also because it was unoccupied. Alternative arrangements of our houses, or different activities within them, will lead to different levels of air pollution.

### 3.4 The contribution of cooking and cleaning activities to overall UK VOC emissions

VOC emissions from households and their relative contribution to the total VOC emissions produced annually in the United Kingdom have not been studied in great detail, compared to the impact from large-scale industrial processes. The UK National Atmospheric Emissions Inventory (NAEI) categorises industrial processes, transport and agricultural emissions of non-methane volatile organic compounds (NMVOCs).<sup>110</sup> In the UK in 2021, 0.78 million tonnes of NMVOCs were emitted in total, primarily from solvent use, industrial processes and transport. Domestic solvent use and food and drink manufacture contributed 0.19 (24%) and 0.12 (15%) million tonnes of NMVOCs to the total respectively.<sup>111</sup>

From our layered day simulation (as described in Section 2.4.1), the total emission rates of NMVOCs from one house following cooking and cleaning activities are 0.56 and 0.13 grams per day respectively. This equates to approximately 205 and 47 grams per year emitted from one house as a result of cooking and cleaning activities respectively (calculation detailed in eqn (S2)†). The cooking emission derives partially from combustion of the gas and partially from the food itself. We assume that the ethane and propane emissions account for the former and the rest of the emissions are from the food (the contribution of propane and ethane to emissions from cooking was approximately 9% for our conditions). Therefore, out of the 204.7 g per year from cooking, we assume that 19.2 g are from burning the gas and 185.5 g are from cooking the food. Note that we are ignoring background emissions of ethane and propane from the pilot light and just focusing on cooking activities.

According to the Office for National Statistics, there are 26.4 million houses in the UK.<sup>112</sup> Therefore, the propane and ethane emissions would equate to 508 tonnes per year from burning gas for cooking (469 and 39 tonnes per year respectively).



According to the Air Quality Expert Group in the UK,<sup>113</sup> 4.01 ktonnes of propane was emitted indoors from residential buildings in 2019. The estimated propane emissions from cooking with gas in our study, are around 13% of the total propane estimated to be emitted from homes in the UK.

Approximately 61.5% of these homes use gas hobs whereas the other 38.5% use electric.<sup>114</sup> We can therefore predict that 61.5% of homes emit 204.7 g per year (3323 tonnes per year) and the other 38.5% emit 185.8 g per year (2080 tonnes per year), giving a total annual emission of 5403 tonnes of NMVOCs emitted outdoors from cooking in UK homes. Similarly, 1229 tonnes are emitted outdoors from cleaning in homes in the UK each year. Based on these assumptions and for the species we have studied, cooking constitutes approximately 0.69% of the total yearly NMVOCs emitted in the UK and cleaning approximately 0.16%. Note that, UK inventory emissions are significantly impacted by sources outside of urban areas, so our values likely underplay the impacts of cooking and cleaning where most of these activities occur.

We can also put these estimated emission rates into context with other sectors. In 2021, road transport in the UK released 23 000 tonnes of NMVOCs.<sup>111</sup> Our household emissions from cooking and cleaning equate to approximately 29% of those released from traffic. Given that vehicle emissions are likely to continue to decline, *e.g.* as the vehicle fleet is electrified, household emissions will become proportionally more important in the future.

### 3.5 Limitations of the study

Although this study aims to understand how indoor sources affect outdoor air pollution, there are some limitations in our methods. The model doesn't account for buoyancy of species once they are released outdoors, especially those emitted from cooking. This should be negligible (even for wood stoves which are much hotter) because the mass of air involved is low. The model also assumes outdoor concentrations of VOCs remain constant, whereas the indoor emissions will enhance them in reality, which will feedback as these pollutants enter other houses. The outdoor VOCs are compiled from a literature search of comprehensive studies performed worldwide, though relatively few exist.<sup>60</sup> Depending on the outdoor VOC concentrations at a location of interest, our findings may have larger or smaller local impacts. The model also uses a one-dimensional airflow scheme, so pollution only travels in one direction along the street. Cooking and cleaning emissions will vary between homes, depending on the meal which is being prepared, the cooking process and fuel used and the type of cleaning product. HOMEChem is still one of the most detailed indoor studies to date, but the cooking emission rates compare reasonably well with more recent, smaller-scale UK studies.<sup>29</sup> In the future, indoor emissions inventories would permit a more detailed exploration of the range of likely emissions indoors from cooking and cleaning activities. Finally, the propane emissions in the HOMEChem study were high owing to emissions from the pilot light.<sup>91</sup> Our results are more representative of gas cooking than electric or induction.

## 4 Conclusions

The aim of this study was to provide a deeper understanding of how cooking and cleaning contribute to indoor air pollution and the subsequent influence they have on the surrounding urban environment. INCHEM-Py has demonstrated the impact that both cooking and cleaning have on secondary indoor chemistry. Chlorine cleaning was much more important for radical chemistry than cooking. The concentrations of OH, HO<sub>2</sub> and RO<sub>2</sub> all increased markedly upon the initiation of cleaning.

We identified some VOCs associated with indoor cooking and cleaning, based on data from the HOMEChem study. Propane and isobutane were good indicators for cooking, and chloroform was a good indicator for bleach cleaning activities. For a row of detached houses, the emissions from each house depend crucially on the activities within those houses and physical parameters such as the air change rate. Emissions can also change depending on the order of activities. For instance, cleaning after cooking suppresses the emission of acetaldehyde.

Our estimated total VOCs from cooking and cleaning indoors is a small proportion of total UK emissions, but that does not mean the impact is negligible because of direct indoor exposures. Even in close proximity to a house(s), near-field VOC concentrations tend to be generally lower than outdoor concentrations, although there is uncertainty in outdoor concentrations of many VOC species. There are generally only limited spatial and temporal measurements of VOCs available. More representative outdoor VOC concentrations would be highly beneficial to better understand the impact of emissions from indoors.

## Author contributions

Toby J. Carter: methodology, software, validation, formal analysis, investigation, data curation, visualisation, writing – original draft, writing – review & editing. David R. Shaw: methodology, software, resources, data curation, writing – review & editing. David C. Carslaw: formal analysis, provision of ADMS data, writing – review & editing. Nicola Carslaw: conceptualisation, methodology, software, validation, writing – original draft, writing – review & editing, supervision, project administration, funding acquisition.

## Conflicts of interest

The authors declare that they have no known competing financial interests or personal relationships that could have appeared to influence the work reported in this paper.

## Acknowledgements

This research is part of MOCCIE 3 (MOdelling Consortium for Chemistry of Indoor Environments), which has received funding from the Alfred P. Sloan Foundation to study Chemistry of Indoor Environments (CIE) (Grant Numbers: G-2018-10083, G-2019-12306 and G-2020-13912). We would like to thank Dr Tim Murrells from Ricardo Energy & Environment (UK) for advice

with UK VOC emissions. Conclusions reached or positions taken by researchers or other grantees represent the views of the grantees themselves and not those of the Alfred P. Sloan Foundation or its trustees, officers, or staff.

## Notes and references

- 1 A. Juginović, M. Vuković, I. Aranza and V. Biloš, Health impacts of air pollution exposure from 1990 to 2019 in 43 European countries, *Sci. Rep.*, 2021, **11**, 22516.
- 2 P. Rafaj, G. Kiesewetter, T. Gül, W. Schöpp, J. Cofala, Z. Klimont, P. Purohit, C. Heyes, M. Amann, J. Borken-Kleefeld and L. Cozzi, Outlook for clean air in the context of sustainable development goals, *Global Environ. Change*, 2018, **53**, 1–11.
- 3 WHO Factfile, <https://www.who.int/news-room/fact-sheets/detail/household-air-pollution-and-health>, Date Accessed: October 2023.
- 4 N. E. Klepeis, W. C. Nelson, W. R. Ott, J. P. Robinson, A. M. Tsang, P. Switzer, J. V. Behar, S. C. Hern and W. H. Engelmann, The National Human Activity Pattern Survey (NHAPS): a resource for assessing exposure to environmental pollutants, *J. Exposure Anal. Environ. Epidemiol.*, 2001, **11**, 231–252.
- 5 A. H. Goldstein, W. W. Nazaroff, C. J. Weschler and J. Williams, How Do Indoor Environments Affect Air Pollution Exposure?, *Environ. Sci. Technol.*, 2021, **55**, 100–108.
- 6 S. Sankhyan, K. Zabinski, R. E. O'Brien, S. Coyan, S. Patel and M. E. Vance, Aerosol emissions and their volatility from heating different cooking oils at multiple temperatures, *Environ. Sci.: Atmos.*, 2022, **2**, 1364–1375.
- 7 R. Tang and C. Pfirang, Indoor particulate matter (PM) from cooking in UK students' studio flats and associated intervention strategies: evaluation of cooking methods, PM concentrations and personal exposures using low-cost sensors, *Environ. Sci.: Atmos.*, 2023, **3**, 537–551.
- 8 K. Kang, H. Kim, D. D. Kim, Y. G. Lee and T. Kim, Characteristics of cooking-generated PM 10 and PM 2.5 in residential buildings with different cooking and ventilation types, *Sci. Total Environ.*, 2019, **668**, 56–66.
- 9 V. Y. Seaman, D. H. Bennett and T. M. Cahill, Indoor acrolein emission and decay rates resulting from domestic cooking events, *Atmos. Environ.*, 2009, **43**, 6199–6204.
- 10 F. Klein, U. Baltensperger, A. S. Prévôt and I. El Haddad, Quantification of the impact of cooking processes on indoor concentrations of volatile organic species and primary and secondary organic aerosols, *Indoor Air*, 2019, **29**, 926–942.
- 11 G. Bekö, C. J. Weschler, A. Wierzbicka, D. G. Karottki, J. Toftum, S. Loft and G. Clausen, Ultrafine particles: exposure and source apportionment in 56 Danish homes, *Environ. Sci. Technol.*, 2013, **47**, 10240–10248.
- 12 C. Wang, B. Bottorff, E. Reidy, C. M. F. Rosales, D. B. Collins, A. Novoselac, D. K. Farmer, M. E. Vance, P. S. Stevens and J. P. Abbatt, Cooking, Bleach Cleaning, and Air Conditioning Strongly Impact Levels of HONO in a House, *Environ. Sci. Technol.*, 2020, **54**, 13488–13497.
- 13 T. D. Nelin, A. M. Joseph, M. W. Gorr and L. E. Wold, Direct and indirect effects of particulate matter on the cardiovascular system, *Toxicol. Lett.*, 2012, **208**, 293–299.
- 14 C. J. Weschler and N. Carslaw, Indoor Chemistry, *Environ. Sci. Technol.*, 2018, **52**, 2419–2428.
- 15 M. S. Waring and J. R. Wells, Volatile organic compound conversion by ozone, hydroxyl radicals, and nitrate radicals in residential indoor air: magnitudes and impacts of oxidant sources, *Atmos. Environ.*, 2015, **106**, 382–391.
- 16 N. Carslaw, A mechanistic study of limonene oxidation products and pathways following cleaning activities, *Atmos. Environ.*, 2013, **80**, 507–513.
- 17 C. F. Marciel Rosales, J. Jiang, A. Lahib, B. P. Bottorff, E. K. Reidy, V. Kumar, A. Tasoglou, H. Huber, S. Dusanter, A. Tomas, B. E. Boor and P. S. Stevens, Chemistry and human exposure implications of secondary organic aerosol production from indoor terpene ozonolysis, *Sci. Adv.*, 2022, **8**, 9156.
- 18 N. Carslaw and D. Shaw, Modification of cleaning product formulations could improve indoor air quality, *Indoor Air*, 2022, **32**, e13021.
- 19 J. Chen, K. H. Møller, P. O. Wennberg and H. G. Kjaergaard, Unimolecular Reactions following Indoor and Outdoor Limonene Ozonolysis, *J. Phys. Chem. A*, 2021, **125**, 669–680.
- 20 M. Kruza, D. Shaw, J. Shaw and N. Carslaw, Towards improved models for indoor air chemistry: a Monte Carlo simulation study, *Atmos. Environ.*, 2021, **262**, 118625.
- 21 P. Wolkoff, P. A. Clausen, C. K. Wilkins and G. D. Nielsen, Formation of strong airway irritants in terpene/ozone mixtures, *Indoor Air*, 2000, **10**, 82–91.
- 22 P. Wolkoff, Indoor air chemistry: terpene reaction products and airway effects, *Int. J. Hyg. Environ. Health*, 2020, **225**, 113439.
- 23 C. Arata, P. K. Misztal, Y. Tian, D. M. Lunderberg, K. Kristensen, A. Novoselac, M. E. Vance, D. K. Farmer, W. W. Nazaroff and A. H. Goldstein, Volatile organic compound emissions during HOMEChem, *Indoor Air*, 2021, **31**, 2099–2117.
- 24 J. H. Ahn, J. E. Szulejko, K. H. Kim, Y. H. Kim and B. W. Kim, Odor and VOC emissions from pan frying of mackerel at three stages: raw, well-done, and charred, *Int. J. Environ. Res. Public Health*, 2014, **11**, 11753–11771.
- 25 K. L. Abdulla, J. M. Delgado-Saborit and R. M. Harrison, Emissions and indoor concentrations of particulate matter and its specific chemical components from cooking: a review, *Atmos. Environ.*, 2013, **71**, 260–294.
- 26 D. C. Zhang, J. J. Liu, L. Z. Jia, P. Wang and X. Han, Speciation of VOCs in the cooking fumes from five edible oils and their corresponding health risk assessments, *Atmos. Environ.*, 2019, **211**, 6–17.
- 27 C. Chen, Y. Zhao and B. Zhao, Emission Rates of Multiple Air Pollutants Generated from Chinese Residential Cooking, *Environ. Sci. Technol.*, 2018, **52**, 1081–1087.



28 K. H. Kim, S. K. Pandey, E. Kabir, J. Susaya and R. J. Brown, The modern paradox of unregulated cooking activities and indoor air quality, *J. Hazard. Mater.*, 2011, **195**, 1–10.

29 H. L. Davies, C. O’Leary, T. J. Dillon, D. R. Shaw, M. D. Shaw, A. Mehra, G. Phillips and N. Carslaw, A measurement and modelling investigation of the indoor air chemistry following cooking activities, *Environ. Sci.: Processes Impacts*, 2023, **25**, 1532–1548.

30 J. J. Schauer, M. J. Kleeman, G. R. Cass and B. R. Simoneit, Measurement of emissions from air pollution sources. 1. C1 through C29 organic compounds from meat charbroiling, *Environ. Sci. Technol.*, 1999, **33**, 1566–1577.

31 F. Klein, S. M. Platt, N. J. Farren, A. Detournay, E. A. Bruns, C. Bozzetti, K. R. Daellenbach, D. Kilic, N. K. Kumar, S. M. Pieber, J. G. Slowik, B. Temime-Roussel, N. Marchand, J. F. Hamilton, U. Baltensperger, A. S. Prévôt and I. El Haddad, Characterization of Gas-Phase Organics Using Proton Transfer Reaction Time-of-Flight Mass Spectrometry: Cooking Emissions, *Environ. Sci. Technol.*, 2016, **50**, 1243–1250.

32 R. A. Wernis, N. M. Kreisberg, R. J. Weber, G. T. Drozd and A. H. Goldstein, Source apportionment of VOCs, IVOCS and SVOCs by positive matrix factorization in suburban Livermore, California, *Atmos. Chem. Phys.*, 2022, **22**, 14987–15019.

33 L. Calderon, R. Maddalena, M. Russell, S. Chen, J. E. Nolan, A. Bradman and K. G. Harley, Air concentrations of volatile organic compounds associated with conventional and “green” cleaning products in real-world and laboratory settings, *Indoor Air*, 2022, **32**, e13162.

34 W. W. Nazaroff and C. J. Weschler, Cleaning products and air fresheners: exposure to primary and secondary air pollutants, *Atmos. Environ.*, 2004, **38**, 2841–2865.

35 S. Zhou, Z. Liu, Z. Wang, C. J. Young, T. C. Vandenboer, B. B. Guo, J. Zhang, N. Carslaw and T. F. Kahan, Hydrogen Peroxide Emission and Fate Indoors during Non-bleach Cleaning: A Chamber and Modeling Study, *Environ. Sci. Technol.*, 2020, **54**, 15643–15651.

36 M. Odabasi, Halogenated volatile organic compounds from the use of chlorine-bleach- containing household products, *Environ. Sci. Technol.*, 2008, **42**, 1445–1451.

37 E. Harding-Smith, D. R. Shaw, M. Shaw, T. J. Dillon and N. Carslaw, Does green mean clean? Volatile organic emissions from regular versus green cleaning products, *Environ. Sci.: Processes Impacts*, 2024, **26**, 436–450.

38 R. E. Dodson, M. Nishioka, L. J. Standley, L. J. Perovich, J. G. Brody and R. A. Rudel, Endocrine disruptors and asthma-associated chemicals in consumer products, *Environ. Health Perspect.*, 2012, **120**, 935–943.

39 K. L. Alford and N. Kumar, Pulmonary health effects of indoor volatile organic compounds—a meta-analysis, *Int. J. Environ. Res. Public Health*, 2021, **18**, 1578.

40 J. Shuai, S. Kim, H. Ryu, J. Park, C. K. Lee, G. B. Kim, V. U. Ultra and W. Yang, Health risk assessment of volatile organic compounds exposure near Daegu dyeing industrial complex in South Korea, *BMC Public Health*, 2018, **18**, 528.

41 M. Medina-Ramón, J. P. Zock, M. Kogevinas, J. Sunyer, Y. Torralba, A. Borrell, F. Burgos and J. M. Antó, Asthma, chronic bronchitis, and exposure to irritant agents in occupational domestic cleaning: a nested case-control study, *Occup. Environ. Med.*, 2005, **62**, 598–606.

42 O. Archangelidi, S. Sathiayajit, D. Consonni, D. Jarvis and S. De Matteis, Cleaning products and respiratory health outcomes in occupational cleaners: a systematic review and meta-analysis, *Occup. Environ. Med.*, 2021, **78**, 541–547.

43 G. W. Hoyle and E. R. Svendsen, Persistent effects of chlorine inhalation on respiratory health, *Ann. N. Y. Acad. Sci.*, 2016, **1378**, 33–40.

44 H. Weill, R. George, M. Schwarz and M. Ziskind, Late evaluation of pulmonary function after acute exposure to chlorine gas, *Am. Rev. Respir. Dis.*, 1969, **99**, 374–379.

45 Health Protection Agency, Chloroform Toxicological Overview, *UK Government Technical Report*, 2007.

46 E. Bingham, B. Cohrssen and C. H. Powell, *Patty’s Toxicology*, Wiley, New York, 5th edn, 2001, vol. 5.

47 Agency for Toxic Substances and Disease Registry (ATSDR), Toxicological Profile for Chloroform, *US Department of Health and Human Services Technical Report*, 1997.

48 D. Y. Leung, Outdoor-indoor air pollution in urban environment: challenges and opportunity, *Front. Environ. Sci.*, 2015, **2**, 1–7.

49 P. M. Shrestha, J. L. Humphrey, E. J. Carlton, J. L. Adgate, K. E. Barton, E. D. Root and S. L. Miller, Impact of outdoor air pollution on indoor air quality in low-income homes during wildfire seasons, *Int. J. Environ. Res. Public Health*, 2019, **16**, 3535.

50 M. F. Link, J. Li, J. C. Ditto, H. Huynh, J. Yu, S. M. Zimmerman, K. L. Rediger, A. Shore, J. P. Abbott, L. A. Garofalo, D. K. Farmer and D. Poppendieck, Ventilation in a Residential Building Brings Outdoor NO<sub>x</sub> Indoors with Limited Implications for VOC Oxidation from NO<sub>3</sub> Radicals, *Environ. Sci. Technol.*, 2023, **57**, 16446–16455.

51 T. V. Vu, G. B. Stewart, N. Kitwiroon, S. Lim, B. Barratt, F. J. Kelly, R. Thompson, R. B. Smith, M. B. Toledoano and S. D. Beavers, Assessing the contributions of outdoor and indoor sources to air quality in London homes of the SCAMP cohort, *Build. Environ.*, 2022, **222**, 109359.

52 B. C. McDonald, J. A. De Gouw, J. B. Gilman, S. H. Jathar, A. Akherati, C. D. Cappa, J. L. Jimenez, J. Lee-Taylor, P. L. Hayes, S. A. McKeen, Y. Y. Cui, S. W. Kim, D. R. Gentner, G. Isaacman-VanWertz, A. H. Goldstein, R. A. Harley, G. J. Frost, J. M. Roberts, T. B. Ryerson and M. Trainer, Volatile chemical products emerging as largest petrochemical source of urban organic emissions, *Science*, 2018, **359**, 760–764.

53 A. Borbon, P. Dominutti, A. Panopoulou, V. Gros, S. Sauvage, M. Farhat, C. Afif, N. Elguindi, A. Fornaro, C. Granier, J. R. Hopkins, E. Liakakou, T. Nogueira, T. Corrêa dos Santos, T. Salameh, A. Armangaud, D. Piga and O. Perrussel, Ubiquity of Anthropogenic Terpenoids in Cities Worldwide: Emission Ratios, Emission Quantification and Implications for Urban Atmospheric



Chemistry, *J. Geophys. Res.: Atmos.*, 2023, **128**, e2022JD037566.

54 G. I. Gkatzelis, M. M. Coggon, B. C. McDonald, J. Peischl, J. B. Gilman, K. C. Aikin, M. A. Robinson, F. Canonaco, A. S. Prevot, M. Trainer and C. Warneke, Observations Confirm that Volatile Chemical Products Are a Major Source of Petrochemical Emissions in U.S. Cities, *Environ. Sci. Technol.*, 2021, **55**, 4332–4343.

55 K. Glojek, G. Močnik, H. D. C. Alas, A. Cuesta-Mosquera, L. Drinovec, A. Gregorič, M. Ogrin, K. Weinhold, I. Ježek, T. Müller, M. Rigler, M. Remškar, D. Van Pinxteren, H. Herrmann, M. Ristorini, M. Merkel, M. Markelj and A. Wiedensohler, The impact of temperature inversions on black carbon and particle mass concentrations in a mountainous area, *Atmos. Chem. Phys.*, 2022, **22**, 5577–5601.

56 R. Sheu, C. F. Fortenberry, M. J. Walker, A. Eftekhari, C. Stönnér, A. Bakker, J. Peccia, J. Williams, G. C. Morrison, B. J. Williams and D. R. Gentner, Evaluating Indoor Air Chemical Diversity, Indoor-to-Outdoor Emissions, and Surface Reservoirs Using High-Resolution Mass Spectrometry, *Environ. Sci. Technol.*, 2021, **55**, 10255–10267.

57 J. M. Mattila, C. Arata, A. Abeleira, Y. Zhou, C. Wang, E. F. Katz, A. H. Goldstein, J. P. Abbatt, P. F. DeCarlo, M. E. Vance and D. K. Farmer, Contrasting Chemical Complexity and the Reactive Organic Carbon Budget of Indoor and Outdoor Air, *Environ. Sci. Technol.*, 2022, **56**, 109–118.

58 A. Eftekhari, C. F. Fortenberry, B. J. Williams, M. J. Walker, A. Dang, A. Pfaff, N. Ercal and G. C. Morrison, Continuous measurement of reactive oxygen species inside and outside of a residential house during summer, *Indoor Air*, 2021, **31**, 1199–1216.

59 D. Shaw and N. Carslaw, INCHEM-Py: an open source Python box model for indoor air chemistry, *J. Open Source Softw.*, 2021, **6**, 3224.

60 D. R. Shaw, T. J. Carter, H. L. Davies, E. Harding-Smith, E. C. Crocker, G. Beel, Z. Wang and N. Carslaw, INCHEM-Py v1.2: a community box model for indoor air chemistry, *Geosci. Model Dev.*, 2023, **16**, 7411–7431.

61 T. J. Carter, D. G. Poppendieck, D. Shaw and N. Carslaw, A Modelling Study of Indoor Air Chemistry: The Surface Interactions of Ozone and Hydrogen Peroxide, *Atmos. Environ.*, 2023, **297**, 119598.

62 G. Beel, B. Langford, N. Carslaw, D. Shaw and N. Cowan, Temperature driven variations in VOC emissions from plastic products and their fate indoors: a chamber experiment and modelling study, *Sci. Total Environ.*, 2023, **881**, 163497.

63 Master Chemical Mechanism (v3.3.1), <https://mcm.york.ac.uk/MCM>, Date Accessed: November 2023.

64 M. E. Jenkin, S. M. Saunders and M. J. Pilling, The tropospheric degradation of volatile organic compounds: a protocol for mechanism development, *Atmos. Environ.*, 1997, **31**, 81–104.

65 S. M. Saunders, M. E. Jenkin, R. G. Derwent and M. J. Pilling, Protocol for the development of the Master Chemical Mechanism, MCM v3 (Part A): tropospheric degradation of non-aromatic volatile organic compounds, *Atmos. Chem. Phys.*, 2003, **3**, 161–180.

66 C. Bloss, V. Wagner, M. E. Jenkin, R. Volkamer, W. J. Bloss, J. D. Lee, D. E. Heard, K. Wirtz, M. Martin-Reviejo, G. Rea, J. C. Wenger and M. J. Pilling, Development of a detailed chemical mechanism (MCMv3.1) for the atmospheric oxidation of aromatic hydrocarbons, *Atmos. Chem. Phys.*, 2005, **5**, 641–664.

67 M. E. Jenkin, S. M. Saunders, V. Wagner and M. J. Pilling, Atmospheric Chemistry and Physics Protocol for the development of the Master Chemical Mechanism, MCM v3 (Part B): tropospheric degradation of aromatic volatile organic compounds, *Atmos. Chem. Phys.*, 2003, **3**, 181–193.

68 M. E. Jenkin, K. P. Wyche, C. J. Evans, T. Carr, P. S. Monks, M. R. Alfara, M. H. Barley, G. B. McFiggans, J. C. Young and A. R. Rickard, Development and chamber evaluation of the MCM v3.2 degradation scheme for  $\beta$ -caryophyllene, *Atmos. Chem. Phys.*, 2012, **12**, 5275–5308.

69 M. E. Jenkin, J. C. Young and A. R. Rickard, The MCM v3.3.1 degradation scheme for isoprene, *Atmos. Chem. Phys.*, 2015, **15**, 11433–11459.

70 M. E. Jenkin, R. Valorso, B. Aumont, M. J. Newland and A. R. Rickard, Estimation of rate coefficients for the reactions of O<sub>3</sub> with unsaturated organic compounds for use in automated mechanism construction, *Atmos. Chem. Phys.*, 2020, **20**, 12921–12937.

71 M. E. Jenkin, R. Valorso, B. Aumont, A. R. Rickard and T. J. Wallington, Estimation of rate coefficients and branching ratios for gas-phase reactions of OH with aromatic organic compounds for use in automated mechanism construction, *Atmos. Chem. Phys.*, 2018, **18**, 9329–9349.

72 M. E. Jenkin, R. Valorso, B. Aumont and A. R. Rickard, Estimation of rate coefficients and branching ratios for reactions of organic peroxy radicals for use in automated mechanism construction, *Atmos. Chem. Phys.*, 2019, **19**, 7691–7717.

73 Z. Wang, D. Shaw, T. Kahan, C. Schoemaecker and N. Carslaw, A modeling study of the impact of photolysis on indoor air quality, *Indoor Air*, 2022, **32**, e13054.

74 N. Carslaw, T. Mota, M. E. Jenkin, M. H. Barley and G. McFiggans, A Significant role for nitrate and peroxide groups on indoor secondary organic aerosol, *Environ. Sci. Technol.*, 2012, **46**, 9290–9298.

75 J. F. Pankow, An absorption model of the gas/aerosol partitioning involved in the formation of secondary organic aerosol, *Atmos. Environ.*, 1994, **28**, 189–193.

76 T. Alapieti, E. Castagnoli, L. Salo, R. Mikkola, P. Pasanen and H. Salonen, The effects of paints and moisture content on the indoor air emissions from pinewood (*Pinus sylvestris*) boards, *Indoor Air*, 2021, **31**, 1563–1576.

77 V. Gallon, P. Le Cann, M. Sanchez, C. Dematteo and B. Le Bot, Emissions of VOCs, SVOCs, and mold during the construction process: contribution to indoor air quality



and future occupants' exposure, *Indoor Air*, 2020, **30**, 691–710.

78 D. A. Missia, E. Demetriou, N. Michael, E. I. Tolis and J. G. Bartzis, Indoor exposure from building materials: a field study, *Atmos. Environ.*, 2010, **44**, 4388–4395.

79 H. Plaisance, J. Vignau-Laulhere, P. Mocho, N. Sauvat, K. Raulin and V. Desauziers, Volatile organic compounds concentrations during the construction process in newly-built timber-frame houses: source identification and emission kinetics, *Environ. Sci.: Processes Impacts*, 2017, **19**, 696–710.

80 C. Yrieix, A. Dulaurent, C. Laffargue, F. Maupetit, T. Pacary and E. Uhde, Characterization of VOC and formaldehyde emissions from a wood based panel: results from an inter-laboratory comparison, *Chemosphere*, 2010, **79**, 414–419.

81 Y. H. Cheng, C. C. Lin and S. C. Hsu, Comparison of conventional and green building materials in respect of VOC emissions and ozone impact on secondary carbonyl emissions, *Build. Environ.*, 2015, **87**, 274–282.

82 P. Harb, N. Locoge and F. Thevenet, Emissions and treatment of VOCs emitted from wood-based construction materials: impact on indoor air quality, *Chem. Eng. J.*, 2018, **354**, 641–652.

83 V. Simon, E. Uitterhaegen, A. Robillard, S. Ballas, T. Véronèse, G. Vilarem, O. Merah, T. Talou and P. Evon, VOC and carbonyl compound emissions of a fiberboard resulting from a coriander biorefinery: comparison with two commercial wood-based building materials, *Environ. Sci. Pollut. Res.*, 2020, **27**, 16121–16133.

84 S. Kim, Control of formaldehyde and TVOC emission from wood-based flooring composites at various manufacturing processes by surface finishing, *J. Hazard. Mater.*, 2010, **176**, 14–19.

85 C. C. Lin, K. P. Yu, P. Zhao and G. Whei-May Lee, Evaluation of impact factors on VOC emissions and concentrations from wooden flooring based on chamber tests, *Build. Environ.*, 2009, **44**, 525–533.

86 J. Nicolle, V. Desauziers, P. Mocho and O. Ramalho, Optimization of FLEC®-SPME for field passive sampling of VOCs emitted from solid building materials, *Talanta*, 2009, **80**, 730–737.

87 A. Manuja, J. Ritchie, K. Buch, Y. Wu, C. M. Eichler, J. C. Little and L. C. Marr, Total surface area in indoor environments, *Environ. Sci.: Processes Impacts*, 2019, **21**, 1384–1392.

88 C. A. McHugh, D. J. Carruthers and H. A. Edmunds, ADMS and ADMS-Urban, *Int. J. Environ. Pollut.*, 1997, **8**, 438–440.

89 ADMS 6, <http://www.cerc.co.uk/environmental-software/ADMS-model.html>, Date Accessed: November 2023.

90 N. Carslaw, A new detailed chemical model for indoor air pollution, *Atmos. Environ.*, 2007, **41**, 1164–1179.

91 D. K. Farmer, M. E. Vance, J. P. Abbatt, A. Abeleira, M. R. Alves, C. Arata, E. Boedicker, S. Bourne, F. Cardoso-Saldaña, R. Corsi, P. F. Decarlo, A. H. Goldstein, V. H. Grassian, L. Hildebrandt Ruiz, J. L. Jimenez, T. F. Kahan, E. F. Katz, J. M. Mattila, W. W. Nazaroff, A. Novoselac, R. E. O'Brien, V. W. Or, S. Patel, S. Sankhyan, P. S. Stevens, Y. Tian, M. Wade, C. Wang, S. Zhou and Y. Zhou, Overview of HOMEChem: House Observations of Microbial and Environmental Chemistry, *Environ. Sci.: Processes Impacts*, 2019, **21**, 1280–1300.

92 E. Reidy, B. P. Bottorff, C. M. F. Rosales, F. J. Cardoso-Saldaña, C. Arata, S. Zhou, C. Wang, A. Abeleira, L. Hildebrandt Ruiz, A. H. Goldstein, A. Novoselac, T. F. Kahan, J. P. Abbatt, M. E. Vance, D. K. Farmer and P. S. Stevens, Measurements of Hydroxyl Radical Concentrations during Indoor Cooking Events: Evidence of an Unmeasured Photolytic Source of Radicals, *Environ. Sci. Technol.*, 2023, **57**, 896–908.

93 M. A. Pothier, E. Boedicker, J. R. Pierce, M. Vance and D. K. Farmer, From the HOMEChem frying pan to the outdoor atmosphere: chemical composition, volatility distributions and fate of cooking aerosol, *Environ. Sci.: Processes Impacts*, 2022, **25**, 314–325.

94 J. M. Mattila, C. Arata, C. Wang, E. F. Katz, A. Abeleira, Y. Zhou, S. Zhou, A. H. Goldstein, J. P. Abbatt, P. F. Decarlo and D. K. Farmer, Dark Chemistry during Bleach Cleaning Enhances Oxidation of Organics and Secondary Organic Aerosol Production Indoors, *Environ. Sci. Technol. Lett.*, 2020, **7**, 795–801.

95 L. Ampollini, E. F. Katz, S. Bourne, Y. Tian, A. Novoselac, A. H. Goldstein, G. Lucic, M. S. Waring and P. F. Decarlo, Observations and Contributions of Real-Time Indoor Ammonia Concentrations during HOMEChem, *Environ. Sci. Technol.*, 2019, **53**, 8591–8598.

96 A. A. Aksенov, J. P. Koelmel, E. Z. Lin, A. V. Melnik, M. E. Vance, D. K. Farmer and K. J. Godri Pollitt, Human Activities Shape Indoor Volatile Chemistry, *Environ. Sci. Technol. Lett.*, 2023, **10**, 965–975.

97 S. Zhou and T. F. Kahan, Spatiotemporal characterization of irradiance and photolysis rate constants of indoor gas-phase species in the UTest house during HOMEChem, *Indoor Air*, 2022, **32**, e12964.

98 Y. Liu, P. K. Misztal, C. Arata, C. J. Weschler, W. W. Nazaroff and A. H. Goldstein, Observing ozone chemistry in an occupied residence, *Proc. Natl. Acad. Sci. U. S. A.*, 2021, **118**, e2018140118.

99 X. Tang, P. K. Misztal, W. W. Nazaroff and A. H. Goldstein, Volatile organic compound emissions from humans indoors, *Environ. Sci. Technol.*, 2016, **50**, 12686–12694.

100 P. Brophy and D. K. Farmer, A switchable reagent ion high resolution time-of-flight chemical ionization mass spectrometer for real-time measurement of gas phase oxidized species: characterization from the 2013 southern oxidant and aerosol study, *Atmos. Meas. Tech.*, 2015, **8**, 2945–2959.

101 Ministry of Housing & Communities & Local Government (UK Government), Ventilation and Indoor Air Quality in New Homes, *Ministry of Housing, Communities and Local Government (United Kingdom), Technical Report*, 2019.

102 W. W. Nazaroff, Residential air-change rates: a critical review, *Indoor Air*, 2021, **31**, 282–313.



103 M. Blocquet, F. Guo, M. Mendez, M. Ward, S. Coudert, S. Batut, C. Hecquet, N. Blond, C. Fittschen and C. Schoemaecker, Impact of the spectral and spatial properties of natural light on indoor gas-phase chemistry: experimental and modeling study, *Indoor Air*, 2018, **28**, 426–440.

104 European Air Quality Portal, <https://eeadmz1-cws-wp-air02.azurewebsites.net/>, Date Accessed: December 2021.

105 M. Kruza and N. Carslaw, How do breath and skin emissions impact indoor air chemistry?, *Indoor Air*, 2019, **29**, 369–379.

106 C. J. Weschler, A. Wisthaler, S. Cowlin, G. Tamás, P. Strøm-Tjensen, A. T. Hodgson, H. Destaillats, J. Herrington, J. Zhang and W. W. Nazaroff, Ozone-initiated chemistry in an occupied simulated aircraft cabin, *Environ. Sci. Technol.*, 2007, **41**, 6177–6184.

107 C. K. Remucal and D. Manley, Emerging investigators series: the efficacy of chlorine photolysis as an advanced oxidation process for drinking water treatment, *Environ. Sci.: Water Res. Technol.*, 2016, **2**, 565–579.

108 O. Setokuchi and M. Sato, Direct dynamics of an alkoxy radical ( $\text{CH}_3\text{O}$ ,  $\text{C}_2\text{H}_5\text{O}$ , and  $\text{i-C}_3\text{H}_7\text{O}$ ) reaction with an oxygen molecule, *J. Phys. Chem. A*, 2002, **106**, 8124–8132.

109 A. C. Davis and J. S. Francisco, Reactivity trends within alkoxy radical reactions responsible for chain branching, *J. Am. Chem. Soc.*, 2011, **133**, 18208–18219.

110 Air Quality Expert Group, Estimation of Changes in Air Pollution Emissions, Concentrations and Exposure during the COVID-19 Outbreak in the UK, *Air Quality Expert Group Technical Report*, 2020.

111 Department for Environment & Food & Rural Affairs, Emissions of Air Pollutants in the UK – Summary, *UK Government Technical Report*, 2023.

112 Office for National Statistics, Housing in England and Wales 2021 Compared with 2011, *Office for National Statistics Technical Report*, 2023.

113 Air Quality Expert Group, Indoor Air Quality, *Department for Environment, Food and Rural Affairs (UK Government) Technical Report*, 2022.

114 Department of Energy & Climate Change, Energy Follow-Up Survey – Report 9: Domestic Appliances, Cooking & Cooling Equipment, *UK Government Technical Report*, 2013.